

## Characterizing concentrated, multiply-scattering and actively-driven fluorescent systems with Confocal Differential Dynamic Microscopy (ConDDM): Supplementary Information

Peter J. Lu (陸述義),<sup>1</sup> Fabio Giavazzi,<sup>2</sup> Thomas E. Angelini,<sup>1</sup> Emanuela Zaccarelli,<sup>3</sup> Frank Jargstorff,<sup>4</sup> Andrew B. Schofield,<sup>5</sup> James N. Wilking,<sup>1</sup> Mark B. Romanowsky,<sup>1</sup> David A. Weitz,<sup>1</sup> and Roberto Cerbino<sup>2</sup>

<sup>1</sup>*Department of Physics and SEAS, Harvard University, Cambridge, Massachusetts 02138, USA*

<sup>2</sup>*Dipartimento di Chimica, Biochimica e Biotecnologie per la Medicina, Università degli Studi di Milano, I-20090, Italy*

<sup>3</sup>*CNR-ISC and Dipartimento di Fisica, Università di Roma La Sapienza, I-00185 Rome, Italy*

<sup>4</sup>*NVIDIA, Santa Clara, California 95050, USA*

<sup>5</sup>*Department of Physics, University of Edinburgh, Edinburgh EH9 3JZ, United Kingdom*

We describe a simple optical model for ConDDM and numerical calculations for evaluating its accuracy in determining the structure factor  $S(q)$  and  $H(q)$  from the short-time behavior of the image structure functions. We show how our procedure leads to accurate determinations of these quantities, even at low values of  $q$ , so long as the particle radius  $a$  is smaller than the thickness of the confocal slice  $\delta z$ .

Following standard treatments [1], we consider the confocal microscope to be a linear, space-invariant system, and therefore write the intensity distribution collected on a two-dimensional detector as:

$$I(\vec{x}, t) = \int d\vec{x}' dz' K(\vec{x} - \vec{x}', -z') c(\vec{x}', z', t) \quad (1)$$

where  $c$  is the fluorophore concentration at the point in 3D realspace  $(x, y, z) \equiv (\vec{x}, z)$  at time  $t$ , and  $K$  is (up to a multiplicative factor) the 3D realspace point-spread function of the microscope [1, 2]. The Fourier-space image correlation function is:

$$\begin{aligned} G(\vec{q}, \delta t) &\equiv \langle I^*(\vec{q}, 0) I(\vec{q}, \delta t) \rangle \quad (2) \\ &= \int dq_z |\tilde{K}(\vec{q}, q_z)|^2 F(\vec{q}, q_z, \delta t) \quad (3) \end{aligned}$$

where  $\tilde{K}(\vec{q}, q_z)$  is the Fourier transform of  $K(\vec{x}, z)$  (i.e., the Fourier-space optical transfer function), and  $F(\vec{q}, q_z, \delta t) = \langle c^*(\vec{q}, q_z, 0) c(\vec{q}, q_z, \delta t) \rangle$  is the unnormalized intermediate scattering function [2, 3]. As in the main text of the paper,  $\vec{q}$  is the 2D wavevector in the plane of the image, so we therefore use capital  $\vec{Q}$  to represent the wavevector in the full 3D reciprocal space:

$$\vec{Q} \equiv (q_x, q_y, q_z) \equiv (\vec{q}, q_z) \quad (4)$$

As described in the main text, the dynamics measured using ConDDM are described by the image structure function  $\Delta(\vec{q}, \delta t)$ , which is related to the image correlation function  $G(\vec{q}, \delta t)$  by:

$$\Delta(\vec{q}, \delta t) = 2[G(\vec{q}, 0) - G(\vec{q}, \delta t)] \quad (5)$$

For a system of  $N$  identical, possibly interacting colloidal particles, the intermediate scattering function is in general a nonexponential function of  $\delta t$ ; however, for short times, as is common in dynamic light scattering (DLS),  $F(Q, \delta t)$  can be approximated with an exponential:

$$F(Q, \delta t) \simeq NP(Q)S(Q)e^{-\delta t/\tau(Q)} \quad (6)$$

This can, in turn, be approximated by the standard expansion:

$$F(Q, \delta t) \simeq NP(Q)S(Q) \left[ 1 - \frac{\delta t}{\tau(Q)} \right] \quad (7)$$

where  $P(Q)$  is the particle form factor,  $S(Q)$  is the structure factor, and  $Q \equiv \vec{Q}^2 = \sqrt{q^2 + q_z^2}$  is the magnitude of the 3D wavevector. The  $Q$ -dependent correlation time,  $\tau(Q)$ , is as in DLS:

$$\tau(Q) = \tau_{\text{dil}} \frac{S(Q)}{H(Q)} \quad (8)$$

where  $\tau_{\text{dil}} = (D_0 q^2)^{-1}$  is the correlation time for a dilute suspension with volume fraction  $\phi_{\text{dil}}$ , such that:

$$S_{\text{dil}} \cong H_{\text{dil}} \cong 1 \quad (9)$$

Substituting,

$$F(Q, \delta t) \simeq NP(Q) \left[ S(Q) - H(Q) \frac{\delta t}{\tau_{\text{dil}}} \right] \quad (10)$$

where  $H(Q)$  is the hydrodynamic factor [4].

Combining Eqs. 3 and 7:

$$G(\vec{q}, \delta t) = N \int dq_z |\tilde{K}(\vec{q}, q_z)|^2 P(Q) \left[ S(Q) - H(Q) \frac{\delta t}{\tau_{\text{dil}}} \right] \quad (11)$$

We rewrite this as:

$$G(q, \delta t) \equiv A(q) \left[ 1 - \frac{\delta t}{\tau(q)} \right] \quad (12)$$

where

$$A(q) = N \int dq_z |\tilde{K}(\vec{q}, q_z)|^2 P(Q) S(Q) \quad (13)$$

and

$$\tau(q) = \tau_{\text{dil}} \frac{\int dq_z |\tilde{K}(\vec{q}, q_z)|^2 P(Q) S(Q)}{\int dq_z |\tilde{K}(\vec{q}, q_z)|^2 P(Q) H(Q)} \quad (14)$$

are extracted from the ConDDM data, as shown in Fig. 1 of the main paper.

For relatively concentrated samples with particle volume fraction  $\phi$ , in the regime where  $\phi_{\text{dil}} \ll \phi < 1$ , the ConDDM-derived experimental structure factor  $S_\phi(q)$  and hydrodynamic factor  $H_\phi(q)$  are given in the main paper:

$$S_\phi(q) = \left( \frac{\phi_{\text{dil}}}{\phi} \right) \frac{A_\phi(q)}{A_{\text{dil}}(q)} \quad (15)$$

$$H_\phi(q) = S_\phi(q) \frac{\tau(q)}{\tau_{\text{dil}}} \quad (16)$$

Substituting,

$$\begin{aligned} S_\phi(q) &= \left( \frac{\phi_{\text{dil}}}{\phi} \right) \frac{A_\phi(q)}{A_{\text{dil}}(q)} \\ &= \frac{\int dq_z |\tilde{K}(\vec{q}, q_z)|^2 P(Q) S_\phi(Q)}{\int dq_z |\tilde{K}(\vec{q}, q_z)|^2 P(Q)} \\ &\equiv \langle S_\phi(Q) \rangle \end{aligned} \quad (17)$$

$$\begin{aligned} H_\phi(q) &= S_\phi(q) \frac{\tau_\phi(q)}{\tau_{\text{dil}}(q)} \\ &= \frac{\int dq_z |\tilde{K}(\vec{q}, q_z)|^2 P(Q) H_\phi(Q)}{\int dq_z |\tilde{K}(\vec{q}, q_z)|^2 P(Q)} \\ &\equiv \langle H_\phi(Q) \rangle \end{aligned} \quad (18)$$

where  $\langle \cdot \rangle$  indicates the expectation value calculated in the normalized distribution:

$$p(q_z; \vec{q}) = \frac{|\tilde{K}(\vec{q}, q_z)|^2 P(Q)}{\int dq_z |\tilde{K}(\vec{q}, q_z)|^2 P(Q)} \quad (19)$$

We calculate eqns. 17 and 18 by using standard theoretical estimates for  $P(Q)$  and  $K$ . For the form factor, we use the standard relation for scattering from a sphere of radius  $R$ :

$$P(Q) = \left[ \frac{3(\sin(QR) - QR \cos(QR))}{(QR)^3} \right]^2 \quad (20)$$

$$= \frac{4\pi}{3} \left( \frac{QR}{2\pi} \right)^{-\frac{3}{2}} J_{3/2}(QR) \quad (21)$$

where  $J_{3/2}$  is the Bessel function of the first kind of order  $3/2$ . For the point-spread function, we use the Gaussian-Lorentzian model:

$$K(\vec{x}, z) = \left[ \frac{\exp\left(-\frac{2x^2}{w_0^2(1+\zeta^2)}\right)}{(1+\zeta^2)} \right]^2 \quad (22)$$

where  $\zeta = \lambda z / \pi n w_0^2$ ,  $n$  is the refractive index,  $w_0$  is the beam waist, and the Stokes shift between illumination and collection wavelengths is neglected, so that  $\lambda$  represents the average of the two wavelengths.

Combining these relations, we calculate numerically the integrals in eqns. 17 and 18 for the conditions of our experiments: particle radius  $a_{\text{PY}} = 0.51 \mu\text{m}$ , volume fractions  $\phi=0.04, 0.09, 0.20, 0.40$ , and confocal slice thickness  $\delta z=1.6$

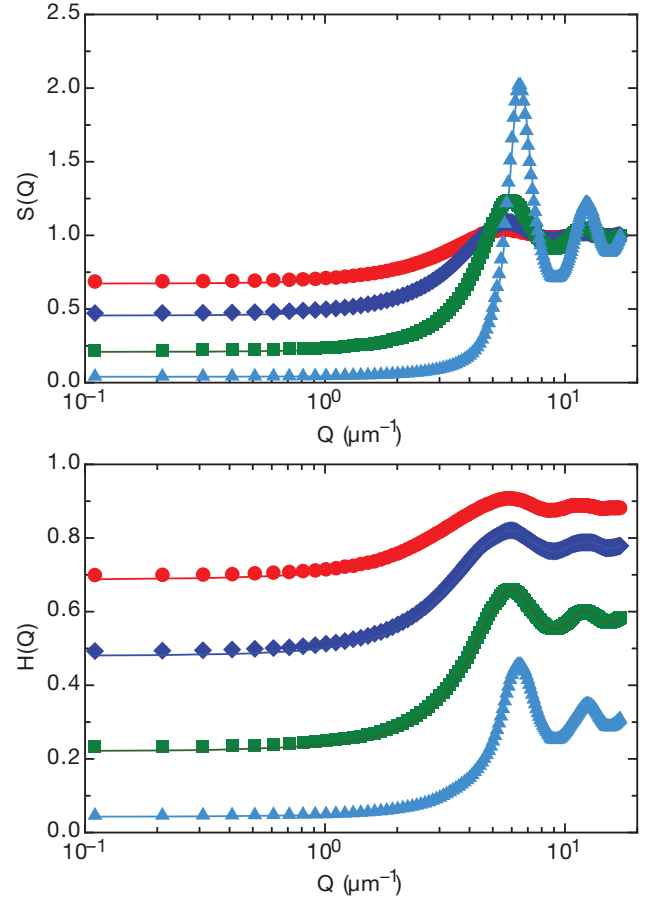


FIG. 1. (color online) Structure factor (top) and hydrodynamic factor (bottom) for colloidal dispersions at various volume fractions (red circles:  $\phi = 0.04$ , blue diamonds:  $\phi = 0.09$ , green squares:  $\phi = 0.20$ , cyan triangles:  $\phi = 0.40$ ). Lines represent the theoretical predictions according to Percus-Yevick (left) and Beenaker-Mazur theories. Symbols are the results of ideal ConDDM experiments obtained by numerical solution of eqn. 17 (top) and eqn. 18 (bottom).

$\mu\text{m}$ . Our numerically calculated  $S(Q)$  and  $H(Q)$  are in excellent agreement with the theoretical estimates of Percus-Yevick, and Beenaker-Mazur, as shown in Fig. 1. This agreement persists through the entire  $Q$ -range relative to our experiment, in particular at low- $Q$ . We explicitly determine the difference between our numerical estimate using the ConDDM framework, and the theoretical prediction, at a low value of  $Q=0.1 \mu\text{m}^{-1}$ , where the dynamics are determined by number fluctuations of particles in the confocal region; the relative differences in  $S(Q)$  are  $2.0 \times 10^{-2}$  ( $\phi = 0.04$ ),  $3.4 \times 10^{-2}$  ( $\phi = 0.09$ ),  $5.0 \times 10^{-2}$  ( $\phi = 0.20$ ), and  $5.2 \times 10^{-2}$  ( $\phi = 0.40$ ). For  $H(Q)$ , the relative errors are  $1.6 \times 10^{-2}$  ( $\phi = 0.04$ ),  $2.6 \times 10^{-2}$  ( $\phi = 0.09$ ),  $4.7 \times 10^{-2}$  ( $\phi = 0.20$ ), and  $7.3 \times 10^{-2}$  ( $\phi = 0.40$ ). In all cases, the agreement is good to within a few percent; furthermore, repeating the calculations for smaller particles improves the agreement. For example, considering particles with half the radius, the largest relative error at  $\phi = 0.40$  for  $S(Q)$  and  $H(Q)$  decreases to  $9.4 \times 10^{-3}$  and

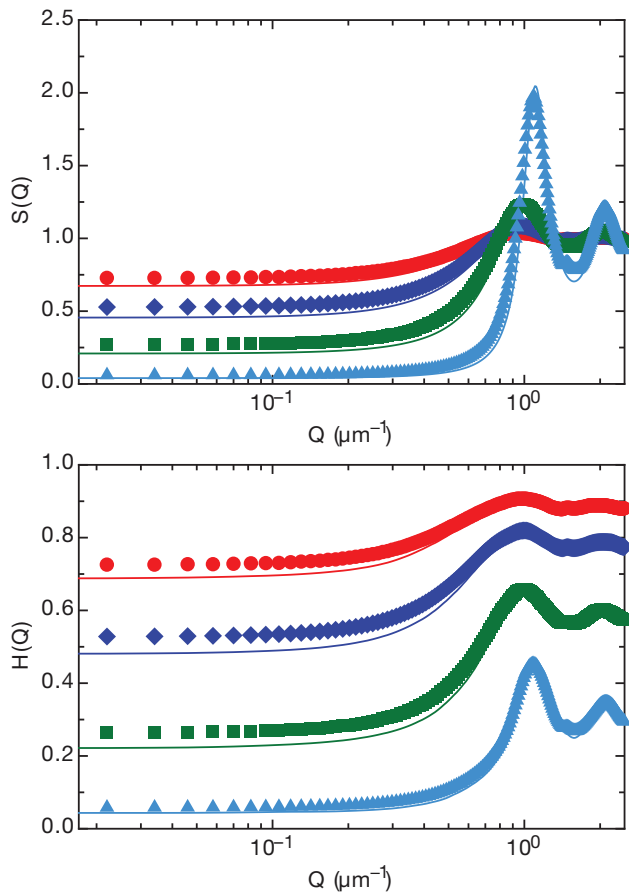


FIG. 2. (color online) Structure factor (top) and hydrodynamic factor (bottom) for colloidal dispersions at various volume fractions (following the colors and symbols of figure 1), but for much larger particles where  $a_{PY} = 3 \mu\text{m}$ . In all cases, the agreement between numerical calculations and theoretical predictions breaks down at low- $q$ .

$2.7 \times 10^{-2}$ , respectively.

There are limits, however, to this agreement. For larger

particles, the numerical calculations of eqns. 17 and 18 begin to deviate from the theoretical predictions, as shown for much larger particles with  $a_{PY} = 3 \mu\text{m}$  in fig. 2. We observe that the quantitative agreement for  $S(Q)$  and  $H(Q)$  persists, so long as the radius of the particle is less than the thickness of the confocal slice:

$$a < \delta z \quad (23)$$

when this condition is met, the particle is small enough that it is observed in the microscope essentially in its entirety. Therefore, so long as the image statistics are sufficient, ConDDM correctly measures the physics of the particle motion, as demonstrated by the calculations shown in fig. 1. However, for particles larger than this limit, only a portion of the particle is observed in confocal microscopy, leading ConDDM to an incorrect estimate of the structure and dynamics, as shown by the calculations in fig. 2.

Therefore, these results demonstrate that, under the conditions relevant to our experiment, the agreement between the ConDDM-derived experimental measurements of  $S(q)$  and  $H(q)$  and the theoretical predictions, as demonstrated in the manuscript, are robust throughout the entire accessible  $q$  range, in particular the low- $q$  limit where  $\tau(q)$  has a plateau. This agreement is inherent to the technique, as shown explicitly with our numerical calculation, and is not an artifact—so long as the particles are smaller than the thickness of the confocal slice (eqn. 23).

- 
- [1] J. Pawley, ed., *Handbook of Biological Confocal Microscopy*, 3rd ed. (Springer, New York, 2008).
  - [2] F. Giavazzi, D. Brogioli, V. Trappe, T. Bellini and R. Cerbino, *Phys. Rev. E* **80**, 031403 (2009).
  - [3] R. Borsali and R. Pecora, *Soft matter: scattering, imaging and manipulation* (Springer, Berlin, 2008).
  - [4] P. N. Segre, O. P. Behrend and P. N. Pusey, *Phys. Rev. E* **52**, 5070 (1995).